crystals

MDPI

Communication

Synthesis and Fluorescence Properties of a Structurally Characterized Hetero-Hexanuclear Zn(II)-La(III) Salamo-Like Coordination Compound Containing Auxiliary Ligands

Wen-Ting Guo [1,2], Ling-Zhi Liu [1], Meng Yu [1], Fei Wang [1], Jian-Chun Ma [1] and Wen-Kui Dong [1,*]

1 School of Chemical and Biological Engineering, Lanzhou Jiaotong University, Lanzhou 730070, China; gwtzy044@126.com (W.-T.G.); llz1009663202@126.com (L.-Z.L.); 18347584353@163.com (M.Y.); wangfei3986@163.com (F.W.); majc0204@126.com (J.-C.M.)

2 Chemical Engineering Department, Jiuquan Vocational Technical College, Jiuquan 735000, China

* Correspondence: dongwk@mail.lzjtu.cn; Tel.: +86-931-493-8703

Received: 11 October 2018; Accepted: 1 November 2018; Published: 4 November 2018

Abstract: A hetero-hexanuclear Zn(II)-La(III) coordination compound, $[\{(ZnL)_2La\}_2(bdc)_2](NO_3)_2$ (H_2bdc = terephthalic acid) has been synthesized with a symmetric Salamo-like bisoxime, and characterized by elemental analyses, IR, UV-Vis, fluorescent spectroscopy, and single-crystal X-ray diffraction analysis. All of the Zn(II) ions are pentacoordinated by N_2O_2 donator atoms from the $(L)^{2-}$ unit and one oxygen atom from one terephthalate anion. The Zn(II) ions adopt trigonal bipyramidal geometries (τ_{Zn1} = 0.61, τ_{Zn2} = 0.56). The La(III) ions are decacoordinated in the Zn(II)-La(III) coordination compound and has a distorted bicapped square antiprism geometry. Meanwhile, the photophysical property of the Zn(II)-La(III) coordination compound was also measured and discussed.

Keywords: Salamo-like bisoxime; Zn(II)-La(III) coordination compound; crystal structure; photophysical property

1. Introduction

Salen-like (*N*,*N*-bis(salicylidene)ethylenediamine) N_2O_2 compounds are a class of the most versatile multidentate chelating ligands and could form stable mono- or multi-nuclear metal coordination compounds with alkaline earth, rare earth, and d-block transition metal ions [1–9]. Salen-like ligands and their corresponding metal coordination compounds have been proverbially studied in recent decades [10–16], these metal coordination compounds are used as precursors to obtain a great deal of oligometallic coordination compounds own to the high coordination abilities [17–21]. In recent years, our research mostly concentrated on the syntheses, crystal structures and properties of Salamo-like (1,2-bis(salicylideneaminooxy)ethane) derivatives and their metal coordination compounds. Salamo-like derivatives are at least 10^4 times more stable than Salen-like ligands due to the unique structures of Salamo-like derivatives [22–24]. When 3-alkoxy groups are introduced of salicylidene moieties, the whole ligand molecule will have an O_4 coordination site besides the N_2O_2 site. The O_4 site of 3-alkoxy Salamo-like derivatives is suitable for alkali metals, alkaline earth metals and rare earth metal ions to obtain heteromulti-nuclear coordination compounds [25–28]. These hetero-metallic Salamo-like coordination compounds have been studied for their catalytic activities [29,30], biological activities [31], and fluorescence properties [32–34]. Meanwhile, supra-molecular chemistry has become increasingly prominent in the coordination

chemistry, for Salamo-like derivatives, supra-molecular structures are formed mainly with the help of hydrogen bonding interactions [35–38]. In our previous studies, a number of Salamo-type derivatives and their hetero-nuclear coordination compounds have been synthesized [39–42]. However, 3d-4f hetero-nuclear Salamo-like coordination compounds containting auxiliary ligands have rarely been reported [43–45].

In order to explore the structures and optical properties of 3d-4f hetero-nuclear metal coordination compounds contained auxiliary ligands, herein the terephtalic acid was selected as a simple multidentate linker owing to its availability and application in the building of Salamo-like Zn(II)-Ln(III) coordination compound. we have successfully designed and synthesized a symmetric Salamo-like derivative H_2L and its corresponding Zn(II)-La(III) coordination compound ($[\{(ZnL)_2La\}_2(bdc)_2](NO_3)_2$). Furthermore, the supra-molecular features and photophysical properties of the Zn(II)-La(III) coordination compound are discussed in detail.

2. Experimental

2.1. Materials and Instrumentation

All chemical reagents were analytical pure reagents, which have not been purified before used. Carbon, nitrogen and hydrogen analyses were obtained using a GmbH VarioEL V3.00 automatic elemental analyzer (Berlin, Germany). Elemental analyses for Zn^{II} and La^{III} were detected by an IRIS ER/S-WP-1 ICP atomic emission spectrometer (Berlin, Germany). Melting points were measured via a microscopic melting point apparatus (Beijing Taike Instrument Limited Company, Beijing, China). ^1H and ^{13}C NMR spectra were recorded in deuterated DMSO solution by German Bruker AVANCE DRX-400 spectroscopy (Bruker AVANCE, Billerica, MA, USA). Infrared spectra were measured with a VERTEX-70 FT-IR spectrophotometer (Bruker, Billerica, MA, USA), with samples prepared as KBr (400–4000 cm^{-1}). UV-Vis absorption and fluorescence spectra were recorded on a Shimadzu UV-2550 (Shimadzu, Japan) and Hitachi F-7000 (Hitachi, Tokyo, Japan) spectrometers, respectively. Quantum yields in solid state were measured using an absolute method by integrating sphere on FLS920 of Edinburgh Instrument. X-ray single crystal structure determination was carried out on a Bruker Smart Apex CCD diffractometer (Bruker AVANCE, Billerica, MA, USA).

2.2. Preparation of Ligand H_2L

Preparation of 1,2-bis(aminooxy)ethane was in accordance with the literature [46,47]. Yield: 71.5%. Anal. Calcd for $C_2H_8N_2O_2$ (%): C, 26.08; H, 8.76; N, 30.42. Found: C, 25.87; H, 8.68; N, 30.51. ^1H NMR (400 MHz, $CDCl_3$) δ 3.79 (s, 4H), 5.52 (s, 4H).

The ligand H_2L was synthesized according to the procedure reported early [43]. Reaction of 1,2-bis(aminooxy)ethane with two equivalents of 3-methoxysalicylaldehyde in ethanol afforded the desired ligand H_2L. The synthesis routes of the Salamo-like bisoxime derivative (H_2L) and its Zn(II)-La(III) coordination compound are shown in Scheme 1. Yield: 81.6%. Mp: 132–134 °C. ^1H NMR (400 MHz, $CDCl_3$) δ 3.87 (s, 6H), 4.46 (s, 4H), 6.81 (dd, J = 7.9, 1.9 Hz, 2H), 6.86 (t, J = 7.9 Hz, 2H), 6.95 (dd, J = 7.9, 1.9 Hz, 2H), 8.23 (s, 2H), 9.70 (s, 2H). ^{13}C NMR (100 MHz, $CDCl_3$) δ 57.4 (CH_3), 72.8 (CH_2), 115.3 (CH), 119.2 (C), 119.6 (CH), 124.1 (CH), 149.5 (C), 150.2 (C), 152.7 (CH=N). IR (KBr, cm^{-1}): 3137 (m) [ν(O–H)], 1601 (m) [ν(C=N)], 1255 (m) [ν(Ar–O)]. Anal. Calcd for $C_{18}H_{20}N_2O_6$ (%): C, 59.99; H, 5.59; N, 7.77. Found: C, 60.07; H, 5.73; N, 7.61%.

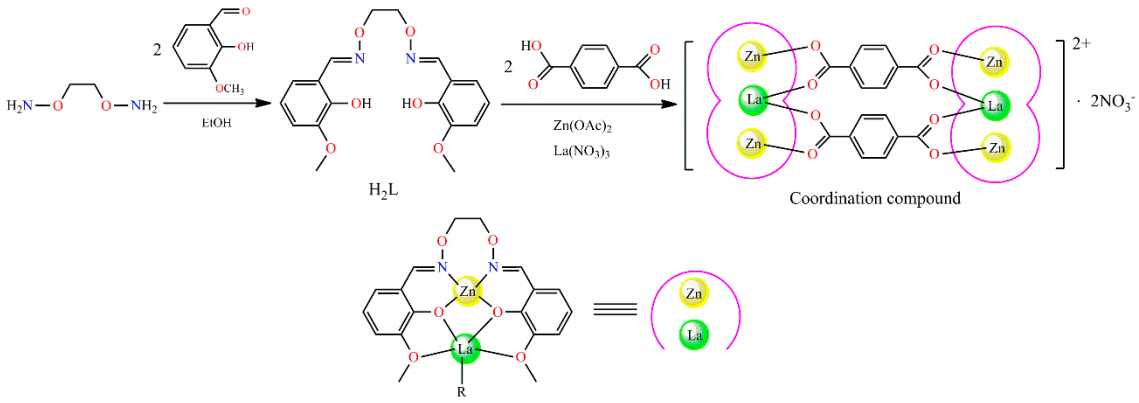

Scheme 1. Synthesis routes of the Salamo-like derivative H_2L and its Zn(II)-La(III) coordination compound.

2.3. Preparation of the Zn(II)-La(III) Coordination Compound

Synthesis route of the Zn(II)-La(III) coordination compound is shown in Scheme 1. To stirring colorless transparent solution of H_2L (15.8 mg, 0.02 mmol) in $CHCl_3$ (3 mL) was added $Zn(OAc)_2{\cdot}2H_2O$ (4.38 mg, 0.02 mmol) and $La(NO_3)_3{\cdot}6H_2O$ (0.02 mmol) in CH_3OH (2 mL). The color of the mixture immediately turns pale yellow and then allowed to mixing with terephthalic acid (0.01 mmol) in CH_3OH (1 mL) and continues stirring for about 30 min at room temperature. After the mixed solution was filtered by absorbent cotton, leaves the filtrate at room temperature for about two weeks. Finally, light-yellow and block-shaped crystals were obtained with the volatilization of solvent. Yield: 60.5%. IR (KBr, cm^{-1}): 1557 (m) [ν(C=N)], 1220 (m) [ν(Ar–O)], 449 (m) [ν(Zn–N)], 529 (m) [ν(Zn–O)]. Anal. Calcd for $C_{88}H_{80}Zn_4La_2N_{10}O_{38}$ (%): C, 43.59; H, 3.33; N, 5.78; Zn, 10.78; La, 11.46. Found: C, 43.71; H, 2.98; N, 5.46; Zn, 10.84; La, 11.39.

2.4. Structure Description of the Zn(II)-La(III) Coordination Compound

Crystal data of the Zn(II)-La(III) coordination compound were collected on a Bruker Smart Apex CCD diffractometer at 173(2) K (Mo-K_α radiation (λ = 0.71073 Å)). The LP factor and Semi-empirical absorption corrections were applied to the intensity data. The structure was solved by the direct methods and refined anisotropically using full-matrix least-squares methods on F^2 with the SHELX-2018 program package. The hydrogen atoms were positioned geometrically and refined isotropically using the 'riding' model (SHELXL-2018). In addition, DELU and AFIX were applied in the structure refinement. The structure contained large in the void couldn't be identified because it was highly disordered and had so small residual peak. Therefore, SQUEEZE in PLATON program was performed to remove the highly disordered solvent. (Solvent Accessible Volume = 914, Electrons Found in S.A.V. = 484). The nonhydrogen atoms were refined anisotropically. Crystal data and structure parameters for the Zn(II)-La(III) coordination compound are given in Table 1. Supplementary crystallographic data for this paper have been deposited at Cambridge Crystallographic Data Centre (1434632) and can be obtained free of charge via www.ccdc.cam.ac.uk/conts/retrieving.html.

Table 1. Crystal data and structure parameters for the Zn(II)-La(III) coordination compound.

Coordination Compound	Zn(II)-La(III)
Empirical formula	$C_{88}H_{80}Zn_4La_2N_{10}O_{38}$
Molecular weight, $g{\cdot}mol^{-1}$	2424.92
Color	Yellow
Crystal size, mm^3	0.15 × 0.12 × 0.06
Habit	Block-shaped
Crystal system	Triclinic
Space group	$P-1$

Table 1. *Cont.*

Coordination Compound	Zn(II)-La(III)
Unit cell dimension	
a (Å)	12.5918(11)
b (Å)	15.9312(15)
c (Å)	16.1881(17)
α (°)	68.980(12)
β (°)	84.083(8)
γ (°)	86.619(9)
V (Å^3)	3014.3(6)
Z	1
Z′	0.5
D_c (g·cm^{-3})	1.336
μ (mm^{-1})	1.550
F(000)	1216
θ Range (°)	1.353–26.022
Index ranges	$-15 \leq h \leq 15$, $-18 \leq k \leq 19$, $0 \leq l \leq 19$
Reflections collected	11813
Completeness (%)	99.4
Data/restraints/parameters	11812/11/644
Final R_1/wR_2 [$I > 2\sigma(I)$]	R_1 = 0.0397, wR_2 = 0.1053
Final R_1/wR_2 (all data)	R_1 = 0.0521, wR_2 = 0.1092
$\Delta\rho_{max/min}$ (e·Å^{-3})	0.715 and −0.626

3. Results and Discussion

3.1. Infrared Spectra

The infrared spectra of H_2L and its Zn(II)-La(III) coordination compound exhibited various bands in the 400–4000 cm^{-1} range (Figure 1). The free ligand H_2L exhibited an obvious characteristic band at 3137 cm^{-1} and can be attributed to the characteristic bands of the OH group. This band was dispeared in the infrared spectrum of the Zn(II)-La(III) coordination compound, indicating the interaction between the OH group and the Zn(II) ion leads to hydroxyl deprotonation [34]. In addition, the free ligand H_2L showed an individual C=N stretching band at 1601 cm^{-1}, while the C=N stretching band of the Zn(II)-La(III) coordination compound appeared at 1557 cm^{-1}. For the ligand H_2L, the Ar-O stretching band appeared at 1255 cm^{-1}, which was observed at 1220 cm^{-1} for the Zn(II)-La(III) coordination compound. The vibration of NO_3^- anion appeared at about 1459 cm^{-1} in the spectrum of the Zn(II)-La(III) coordination compound. The C=N and Ar–O stretching frequencies are shifted, indicating the formation of new chemical bonds (Zn–O and Zn–N) [25]. For the Zn(II)-La(III) coordination compound, the ν(Zn–O) and ν(Zn–N) frequencies were observed at 449 and 529 cm^{-1}, respectively. Just as *Percy* and *Thornton* suggested [48], the M-O and M-N stretching frequency assignments are difficult sometimes.

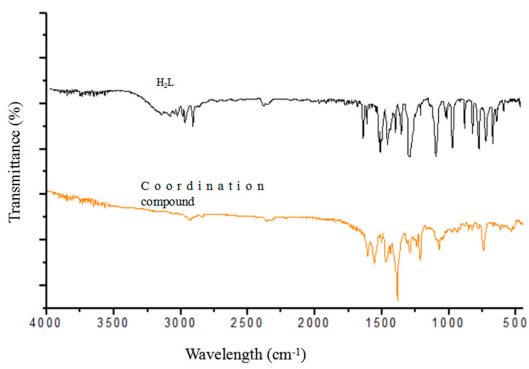

Figure 1. The infrared spectra of the ligand H_2L and its Zn(II)-La(III) coordination compound.

3.2. UV-Vis Spectra

The UV-Vis spectra of H_2L and its Zn(II)-La(III) coordination compound were measured in 1×10^{-5} mol·L^{-1} CH_2Cl_2 solution in freshly prepared solution are obtained in the range of 200–450 nm at room temperature, as shown in Figure 2. As can be seen from the diagram, the absorption peak of the Zn(II)-La(III) coordination compound is evidently different from the ligand before coordination. The absorption spectrum of H_2L showed that two relatively strong absorption peaks appeared at ca. 266 nm ($\varepsilon = 1.8 \times 10^4$ M^{-1}·cm^{-1}) and 322 nm ($\varepsilon = 6.1 \times 10^3$ M^{-1}·cm^{-1}), which can be attributed to π-π* transitions of the benzene rings and the C=N bonds [17]. Compared with the free ligand H_2L, the corresponding absorption peak of the Zn(II)-La(III) coordination compound appeared at ca. 278 nm ($\varepsilon = 4.1 \times 10^4$ M^{-1}·cm^{-1}) was remarkably red shifted upon coordination to metal ions. The absorption peak at ca. 322 nm is absent in the Zn(II)-La(III) coordination compound. Meanwhile, a new absorption peak appeared at ca. 349 nm ($\varepsilon = 1.2 \times 10^4$ M^{-1}·cm^{-1}) in the Zn(II)-La(III) coordination compound that might be owing to M→L (MLCT) charge-transfer transition, which is characteristic of the transition metal coordination compound with N_2O_2 coordination spheres [27].

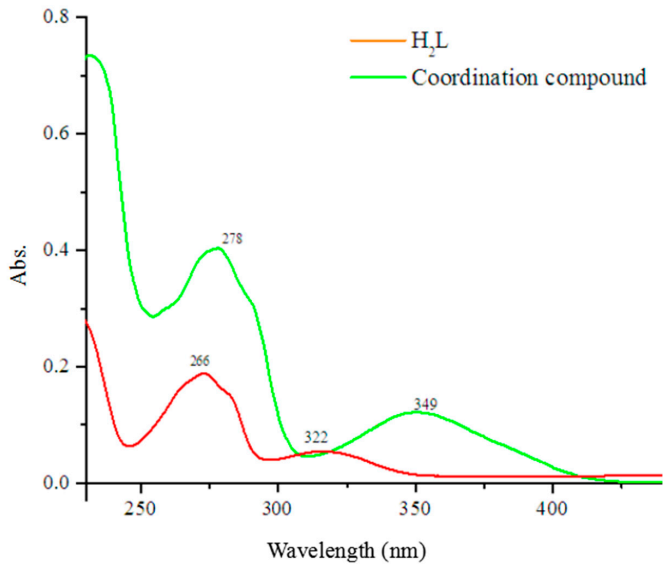

Figure 2. UV-Vis spectra of H_2L and its Zn(II)-La(III) coordination compound.

3.3. Crystal Structure of Zn(II)-La(III) Coordination Compound

Crystal structure of the Zn(II)-La(III) coordination compound exhibited a symmetric hexanuclear structure, which is different from the common trinuclear bis(salamo)-type coordination compounds reported earlier [43,46]. The crystal structure of the Zn(II)-La(III) coordination compound and the coordination polyhedra of metal atoms are shown in Figure 3. Essential bond lengths and angles are listed in Table 2.

Table 2. Essential bond lengths (Å) and angles (°) for the Zn(II)-La(III) coordination compound.

Bond		Bond		Bond	
La1–O13	2.459(3)	La1–O1	2.720(3)	O14–Zn1	1.998(3)
La1–O16 #1	2.497(3)	La1–O12	2.781(3)	O5–Zn1	2.055(3)
La1–O8	2.506(2)	La1–O6	2.813(3)	N4–Zn2	1.992(4)
La1–O5	2.519(3)	La1–Zn1	3.5369(7)	N3–Zn2	2.122(3)
La1–O11	2.523(3)	La1–Zn2	3.5491(7)	O8–Zn2	1.976(3)
La1–O2	2.536(3)	N1–Zn1	2.132(3)	O11–Zn2	2.065(3)
La1–O7	2.690(3)	N2–Zn1	2.034(4)	O15–Zn2 #1	1.984(3)

Table 2. *Cont.*

Bond		Bond		Bond	
Angles		Angles		Angles	
O13–La1–O16 #1	75.54(9)	O5–La1–O2	62.63(9)	O12–La1–O6	161.99(9)
O13–La1–O8	152.43(9)	O11–La1–O2	118.54(9)	O2–Zn1–O14	113.20(13)
O16 #1–La1–O8	76.91(9)	O13–La1–O7	139.64(9)	O2–Zn1–N2	126.73(13)
O13–La1–O5	70.42(9)	O16 #1–La1–O7	123.92(9)	O14–Zn1–N2	119.87(14)
O16 #1–La1–O5	107.80(9)	O8–La1–O7	59.53(9)	O2–Zn1–O5	81.13(11)
O8–La1–O5	118.12(9)	O5–La1–O7	69.87(9)	O14–Zn1–O5	99.14(11)
O13–La1–O11	108.48(9)	O11–La1–O7	111.38(9)	N2–Zn1–O5	86.31(13)
O16 #1–La1–O11	70.54(9)	O2–La1–O7	81.02(8)	O2–Zn1–N1	86.92(13)
O8–La1–O11	62.21(9)	O13–La1–O1	122.61(9)	O14–Zn1–N1	96.36(12)
O5–La1–O11	178.28(9)	O16 #1–La1–O1	142.29(9)	N2–Zn1–N1	91.52(14)
O13–La1–O2	74.77(9)	O8–La1–O1	80.96(8)	O5–Zn1–N1	163.23(12)
O16 #1–La1–O2	150.28(9)	O5–La1–O1	109.50(9)	O8–Zn2–O15 #1	112.61(12)
O8–La1–O2	132.80(9)	O11–La1–O1	72.20(9)	O8–Zn2–N4	130.16(15)
O7–La1–O1	66.05(9)	O2–La1–O1	58.53(9)	O15 #1–Zn2–N4	116.62(15)
O11–La1–O12	58.19(8)	O13–La1–O12	67.16(10)	O8–Zn2–O11	79.99(11)
O2–La1–O12	69.32(9)	O16 #1–La1–O12	97.93(9)	O15 #1–Zn2–O11	97.48(11)
O7–La1–O12	132.07(9)	O8–La1–O12	117.95(9)	N4–Zn2–O11	86.41(14)
O1–La1–O12	66.44(9)	O5–La1–O12	121.99(8)	O8–Zn2–N3	87.90(14)
O13–La1–O6	97.96(9)	O7–La1–O6	65.84(8)	O15 #1–Zn2–N3	97.41(12)
O16 #1–La1–O6	67.47(9)	O1–La1–O6	131.57(8)	N4–Zn2–N3	93.10(15)
O8–La1–O6	70.46(9)	O11–La1–O6	121.87(8)	O11–Zn2–N3	163.57(13)
O5–La1–O6	57.34(8)	O2–La1–O6	118.01(9)		

Symmetry transformations used to generate equivalent atoms: #1 $-x+2, -y+1, -z$.

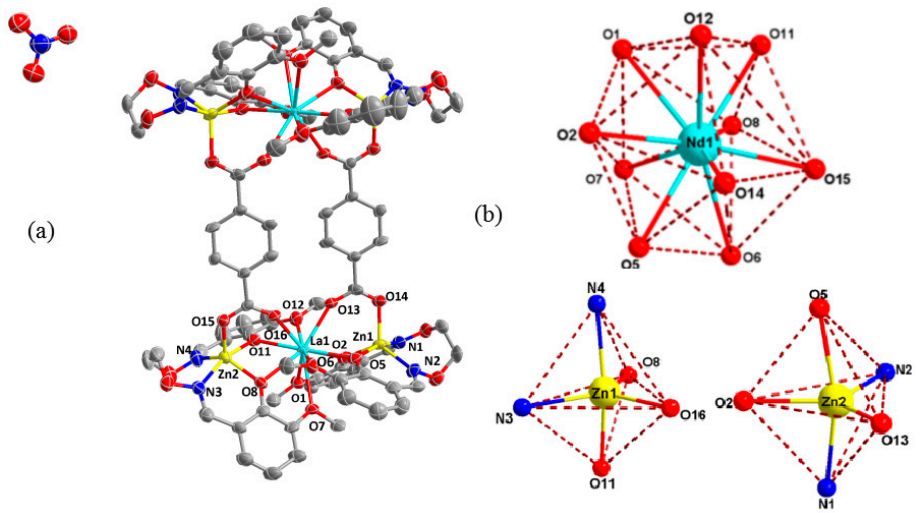

Figure 3. (**a**) Crystal structure of the Zn(II)-La(III) coordination compound (hydrogen atoms are omitted in structure). (**b**) Coordination polyhedra for metal atoms of the Zn(II)-La(III) coordination compound.

The Zn(II)-La(III) coordination compound crystallizes in the triclinic crystal system, space group $P-1$ and the unit cell contains four Zn(II) ions, four $(L)^{2-}$ units, two $(bdc)^{2-}$ ions, two La(III) ions, and two free NO_3^- ions. The Zn(II)-La(III) coordination compound was assembled by two trinuclear units $[(ZnL)_2La]$ and two terephthalic acid, similar to the Zn(II)-Ln(III) coordination compounds reported [49].

In the crystal structure of the Zn(II)-La(III) coordination compound, each Zn(II) ion is located in the N_2O_2 coordination cavity, which have pentacoordinate environments, and the axial position is occupied by one oxygen atom of terephthalic acid. The four Zn(II) ions assumes a distorted trigonal

bipyramidal geometries, which were inferred by calculating the value of τ_{Zn1} = 0.61, τ_{Zn2} = 0.56, respectively [50]. The La(III) ions have a decacoordinate environment, consisting of eight oxygen atoms (O1, O2, O5, O6, O7, O8, O11, and O12) come from two deprotonation $(L)^{2-}$ units, two oxygen atoms (O13 and O16) of two terephthalic acid. Thus, all of the La(III) ions adopt a distorted bicapped square antiprism geometry.

The hydrogen bonding interactions are listed in Table 3. In the crystal structure of the Zn(II)-La(III) coordination compound, the molecular structure is stabilized through intramolecular C-H···O interactions (C9-H9B···O14, C18-H18B···O16, C27-H27B···O15, and C36-H36B···O13) (Figure 4). Intermolecular interactions, especially classical and non-classical hydrogen bonds, are playing a crucial role in the formation of crystalline solids and their physiochemical properties [51–59]. There are two inter-molecular C29-H29···O10$^{\#}$ and C31-H31···O18 hydrogen bonding interactions, which can link each cell unit through inter-molecular hydrogen bondings (Figure 5). Additionally, the hydrogen bonding scheme of the Zn(II)-La(III) coordination compound is defective owing to suppression of the electron density originating from solvent molecules (used SQUEEZE) and subsequent exclusion of these solvent molecules from the refinement model.

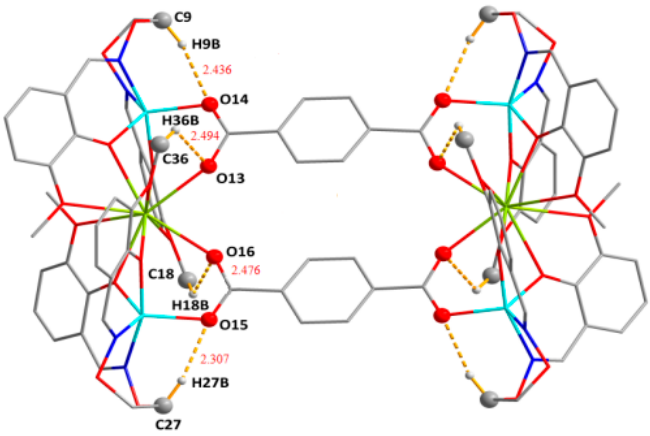

Figure 4. Intramolecular hydrogen bonding interactions of the Zn(II)-La(III) coordination compound (hydrogen atoms, except those forming hydrogen bonds, are omitted for clarity).

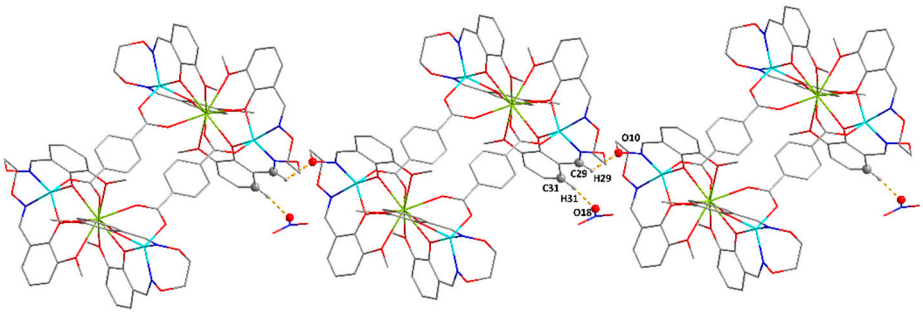

Figure 5. The one-dimensional structure of the Zn(II)-La(III) coordination compound with intermolecular hydrogen bondings (hydrogen atoms have been omitted except those formation of hydrogen bonds).

Table 3. Putative hydrogen bonding interactions (Å, °) for the Zn(II)-La(III) coordination compound.

D-X···A	d(D-X)	d(X···A)	d(D···A)	∠DXA	Symmetry Code
C9-H9B···O14	0.99	2.44	3.322(5)	149	
C18-H18B···O16	0.98	2.48	3.098(5)	121	
C27-H27B···O15	0.99	2.31	3.239(6)	156	
C29-H29···O10	0.95	2.40	3.011(7)	122	$1-x, 2-y, -z$
C31-H31···O18	0.95	1.81	2.748(8)	169	$x, 1+y, -1+z$
C36-H36B···O13	0.98	2.49	3.122(6)	122	

3.4. Fluorescence Properties

The fluorescence properties of H_2L and its Zn(II)-La(III) coordination compound were researched at room temperature (Figure 6).

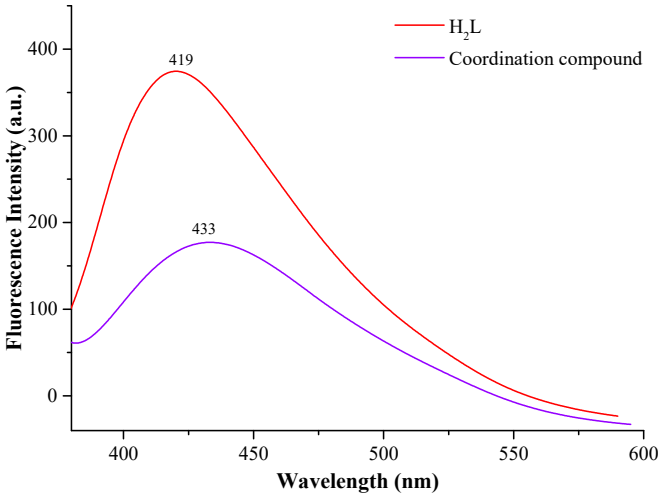

Figure 6. Emission spectra of H_2L (c = 1 × 10^{-5} M, λ_{ex} = 360 nm) and its Zn(II)-La(III) coordination compound.

With excitation at 360 nm, the free ligand H_2L showed strong emission peak at about 419 nm, which can be attributed to the intra-ligand π-π^* transition. Similarly, the Zn(II)-La(III) coordination compound also exhibited an intense luminescence with maximum emission at ca. 433 nm and the emission quantum yield Φ = 0.19% [49]. Compared with the ligand H_2L, the fluorescence intensity of the Zn(II)-La(III) coordination compound showed a marked reduction, indicating that the addition of metal ions induced the change of fluorescence characteristics of the ligand; it is further explained that the (Zn/L)-center has absorbed and transferred energy to La(III) ion as a type of metal-organic antenna [43].

4. Conclusions

We have designed and synthesized a symmetric Salamo-like bioxime ligand H_2L, and obtained a hetero-hexanuclear Zn(II)-La(III) coordination compound $[\{(ZnL)_2La\}_2(bdc)_2](NO_3)_2$. The crystal structure of the Zn(II)-La(III) coordination compound showed that all of the Zn(II) ions have pentacoordinate environments and adopt distorted trigonal bipyramidal geometries. The La(III) ions adopt a distorted bicapped square antiprism geometry. The fluorescence behavior of H_2L and its Zn(II)-La(III) coordination compounds was studied, compared with the ligand H_2L, the fluorescence intensity of the Zn(II)-La(III) coordination compound showed a marked reduction, indicating that the addition of Zn(II)-La(III) ions induced the change of fluorescence characteristics.

Author Contributions: W.-K.D. conceived and designed the experiments; W.-T.G. and J.-C.M. performed the experiments; F.W. and Y.Z. analyzed the data; L.-Z.L. and M.Y. wrote the paper. W.-K.D. contributed reagents/materials/analysis tools.

Funding: This research were funded by the National Natural Science Foundation of China (21761018) and the Program for Excellent Team of Scientific Research in Lanzhou Jiaotong University (201706).

Acknowledgments: This work was supported by the National Natural Science Foundation of China (21761018) and the Program for Excellent Team of Scientific Research in Lanzhou Jiaotong University (201706), which is gratefully acknowledged.

Conflicts of Interest: The authors declare no competing financial interests.

References

1. Zhou, J.J.; Song, X.Q.; Liu, Y.A.; Wang, X.L. Substituent-tuned structure and luminescence sensitizing towards Al^{3+} based on phenoxy bridged dinuclear Eu^{III} complexes. *RSC Adv.* **2017**, *7*, 25549–25559. [CrossRef]
2. Akine, S. Novel ion recognition systems based on cyclic and acyclic oligo(salen)-type ligands. *J. Incl. Phenom. Macrocycl. Chem.* **2012**, *72*, 25–54. [CrossRef]
3. Akine, S.; Varadi, Z.; Nabeshima, T. Synthesis of planar metal complexes and the ctacking abilities of naphthalenediol-based acyclic and macrocyclic Salen-type ligands. *Eur. J. Inorg. Chem.* **2013**, 5987–5998. [CrossRef]
4. Che, C.M.; Huang, J.S. Metal complexes of chiral binaphthyl Schiff-base ligands and their application in stereoselective organic transformations. *Coord. Chem. Rev.* **2003**, *242*, 97–113. [CrossRef]
5. Song, X.Q.; Cheng, G.Q.; Wang, X.R.; Xu, W.Y.; Liu, P.P. Structure-based description of a step-by-step synthesis of heterodinuclear $Zn^{II}Ln^{III}$ complexes and their luminescence properties. *Inorg. Chim. Acta* **2015**, *425*, 145–153. [CrossRef]
6. Chai, L.Q.; Huang, J.J.; Zhang, H.S. An unexpected cobalt (III) complex containing a schiff base ligand: Synthesis, crystal structure, spectroscopic behavior, electrochemical property and SOD-like activity. *Spectrochim. Acta Part A* **2014**, *131*, 526–530. [CrossRef] [PubMed]
7. Chai, L.Q.; Huang, J.J.; Zhang, J.Y.; Li, Y.X. Two 1-D and 2-D cobalt(II) complexes: Synthesis, crystal structures, spectroscopic and electrochemical properties. *J. Coord. Chem.* **2015**, *68*, 1224–1237. [CrossRef]
8. Chai, L.Q.; Tang, L.J.; Chen, L.C.; Huang, J.J. Structural, spectral, electrochemical and DFT studies of two mononuclear manganese(II) and zinc(II) complexes. *Polyhedron* **2017**, *122*, 228–240. [CrossRef]
9. Chai, L.Q.; Zhang, K.Y.; Tang, L.J.; Zhang, J.Y.; Zhang, H.S. Two mono- and dinuclear Ni(II) complexes constructed from quinazoline-type ligands: Synthesis, x-ray structures, spectroscopic, electrochemical, thermal, and antimicrobial studies. *Polyhedron* **2017**, *130*, 100–107. [CrossRef]
10. Chen, C.Y.; Zhang, J.W.; Zhang, Y.H.; Yang, Z.H.; Wu, H.L. Gadolinium(III) and dysprosium(III) complexes with a schiff base bis(*N*-salicylidene)-3-oxapentane-1,5-diamine: Synthesis, characterization, antioxidation, and DNA-binding studies. *J. Coord. Chem.* **2015**, *68*, 1054–1071. [CrossRef]
11. Wu, H.L.; Pan, G.L.; Bai, Y.C.; Wang, H.; Kong, J. Synthesis, structure, antioxidation, and DNA-bindingstudies of a binuclear ytterbium(III) complex with bis(N-salicylidene)-3-oxapentane-1,5-diamine. *Res. Chem. Intermed.* **2015**, *41*, 3375–3388. [CrossRef]
12. Wu, H.L.; Bai, Y.C.; Zhang, Y.H.; Pan, G.L.; Kong, J.; Shi, F.; Wang, X.L. Two lanthanide(III) complexes based on the schiff base *N*,*N*-Bis(salicylidene)-1,5-diamino-3-oxapentane: Synthesis, characterization, DNA-binding properties, and antioxidation. *Z. Anorg. Allg. Chem.* **2014**, *640*, 2062–2071. [CrossRef]
13. Wu, H.L.; Bai, Y.C.; Zhang, Y.H.; Li, Z.; Wu, M.C.; Chen, C.Y.; Zhang, J.W. Synthesis, crystal structure, antioxidation and DNA-binding properties of a dinuclear copper(II) complex with bis(N-salicylidene)-3-oxapentane-1,5-diamine. *J. Coord. Chem.* **2014**, *67*, 3054–3066. [CrossRef]
14. Wu, H.L.; Pan, G.L.; Bai, Y.C.; Zhang, Y.H.; Wang, H.; Shi, F.R.; Wang, X.L.; Kong, J. Study on synthesis, crystal structure, antioxidant and DNA-binding of mono-, di-and poly-nuclear lanthanides complexes with bis (N-salicylidene)-3-oxapentane-1, 5-diamine. *J. Photochem. Photobiol. B* **2014**, *135*, 33–43. [CrossRef] [PubMed]
15. Wu, H.L.; Pan, G.L.; Bai, Y.C.; Wang, H.; Kong, J.; Shi, F.R.; Zhang, Y.H.; Wang, X.L. Preparation, structure, DNA-binding properties, and antioxidant activities of a homodinuclear erbium(III) complex with a pentadentate schiff base ligand. *J. Chem. Res.* **2014**, *38*, 211–217. [CrossRef]
16. Wu, H.L.; Wang, C.P.; Wang, F.; Peng, H.P.; Zhang, H.; Bai, Y.C. A new manganese(III) complex from bis(5-methylsalicylaldehyde)-3-oxapentane-1,5-diamine: Synthesis, characterization, antioxidant activity and luminescence. *J. Chin. Chem. Soc.* **2015**, *62*, 1028–1034. [CrossRef]
17. Song, X.Q.; Liu, P.P.; Wang, C.Y.; Liu, Y.A.; Liu, W.S.; Zhang, M. Three sandwich-type zinc(II)–lanthanide(III) clusters: Structures, luminescence and magnetic properties. *RSC Adv.* **2017**, *7*, 22692–22698. [CrossRef]
18. Sun, Y.X.; Wang, L.; Dong, X.Y.; Ren, Z.L.; Meng, W.S. Synthesis, characterization, and crystal structure of a supramolecular Co^{II} complex containing Salen-type bisoxime. *Synth. React. Inorg. Metal-Org. Nano-Metal Chem.* **2013**, *43*, 599–603. [CrossRef]

19. Sun, Y.X.; Xu, L.; Zhao, T.H.; Liu, S.H.; Dong, X.T. Synthesis and crystal structure of a 3D supramolecular copper(II) complex with 1-(3-{[(E)-3-bromo-5-chloro-2-hydroxybenzylidene]amino}phenyl) ethanone oxime. *Synth. React. Inorg. Metal-Org. Nano-Metal Chem.* **2013**, *43*, 509–513. [CrossRef]
20. Sun, Y.X.; Zhang, S.T.; Ren, Z.L.; Dong, X.Y.; Wang, L. Synthesis, characterization, and crystal structure of a new supramolecular Cd^{II} complex with halogen-substituted Salen-type bisoxime. *Synth. React. Inorg. Metal-Org. Nano-Metal Chem.* **2013**, *43*, 995–1000. [CrossRef]
21. Sun, Y.X.; Gao, X.H. Synthesis, characterization, and crystal structure of a new Cu^{II} complex with Salen-type ligand. *Synth. React. Inorg. Metal-Org. Nano-Metal Chem.* **2011**, *41*, 973–978. [CrossRef]
22. Akine, S.; Taniguchi, T.; Nabeshima, T. Synthesis and characterization of novel ligands 1,2-bis(salicylideneaminooxy)ethanes. *Chem. Lett.* **2001**, *30*, 682–683. [CrossRef]
23. Akine, S.; Utsuno, F.; Taniguchi, T.; Nabeshima, T. Dinuclear complexes of the N_2O_2 oxime chelate ligand with zinc(II)–lanthanide(III) as a selective sensitization system for Sm^{3+}. *Eur. J. Inorg. Chem.* **2010**, *49*, 3143–3152. [CrossRef]
24. Dong, Y.J.; Li, X.L.; Zhang, Y.; Dong, W.K. A highly selective visual and fluorescent sensor for Pb^{2+} and Zn^{2+} and crystal structure of Cu^{2+} complex based-on a novel single-armed Salamo-type bisoxime. *Supramol. Chem.* **2017**, *29*, 518–527. [CrossRef]
25. Chen, L.; Dong, W.K.; Zhang, H.; Zhang, Y.; Sun, Y.X. Structural variation and luminescence properties of triand dinuclear Cu^{II} and Zn^{II} complexes constructed from a naphthalenediol-based bis(Salamo)-type ligand. *Cryst. Growth Des.* **2017**, *17*, 3636–3648. [CrossRef]
26. Sun, Y.X.; Liu, L.Z.; Wang, F.; Shang, X.Y.; Chen, L.; Dong, W.K. Structural and hirshfeld surface analyses of a novel hetero-tetranuclear Cu^{II}-Na^{I} bis(Salamo)-based coordination compound. *Crystals* **2018**, *8*, 227. [CrossRef]
27. Zhang, L.W.; Li, X.Y.; Kang, Q.P.; Liu, L.Z.; Ma, J.C.; Dong, W.K. Structures and fluorescent and magnetic behaviors of newly synthesized Ni^{II} and Cu^{II} coordination compounds. *Crystals* **2018**, *8*, 173. [CrossRef]
28. Akine, S.; Kagiyama, S.; Nabeshima, T. Modulation of multimetal complexation behavior of tetraoxime ligand by covalent transformation of olefinic functionalities. *Inorg. Chem.* **2010**, *49*, 2141–2152. [CrossRef] [PubMed]
29. Li, L.H.; Dong, W.K.; Zhang, Y.; Akogun, S.F.; Xu, L. Syntheses, structures and catecholase activities of homo- and hetero-trinuclear cobalt(II) complexes constructed from an acyclic naphthalenediol-based bis(Salamo)-type ligand. *Appl. Organomet. Chem.* **2017**, *31*, e3818. [CrossRef]
30. Li, X.Y.; Chen, L.; Gao, L.; Zhang, Y.; Akogun, S.F.; Dong, W.K. Syntheses, crystal structures and catalytic activities of two solvent-induced homotrinuclear Co(II) complexes with a naphthalenediol-based bis(Salamo)-type tetraoxime ligand. *RSC Adv.* **2017**, *7*, 35905–35916. [CrossRef]
31. Wang, L.; Hao, J.; Zhai, L.X.; Zhang, Y.; Dong, W.K. Synthesis, crystal structure, luminescence, electrochemical and antimicrobial properties of bis(Salamo)-based Co(II) complex. *Crystals* **2017**, *7*, 277. [CrossRef]
32. Wang, B.J.; Dong, W.K.; Zhang, Y.; Akogun, S.F. A novel relay-sensor for highly sensitive and selective detection of Zn^{2+}/Pic^{-} and fluorescence on/off switch response of H^{+}/OH^{-}. *Sens. Actuators B* **2017**, *247*, 254–264. [CrossRef]
33. Dong, W.K.; Li, X.L.; Wang, L.; Zhang, Y.; Ding, Y.J. A new application of Salamo-type bisoximes: As a relay-sensor for Zn^{2+}/Cu^{2+} and its novel complexes for successive sensing of H^{+}/OH^{-}. *Sens. Actuators B* **2016**, *229*, 370–378. [CrossRef]
34. Zheng, S.S.; Dong, W.K.; Zhang, Y.; Chen, L.; Ding, Y.J. Four Salamo-type 3d–4f hetero-bimetallic $[Zn^{II}Ln^{III}]$ complexes: Syntheses, crystal structures, and luminescent and magnetic properties. *New J. Chem.* **2017**, *41*, 4966–4973. [CrossRef]
35. Dong, Y.J.; Dong, X.Y.; Dong, W.K.; Zhang, Y.; Zhang, L.S. Three asymmetric Salamo-type copper(II) and cobalt(II) complexes: Syntheses, structures, fluorescent properties. *Polyhedron* **2017**, *123*, 305–315. [CrossRef]
36. Dong, X.Y.; Li, X.Y.; Liu, L.Z.; Zhang, H.; Ding, Y.J.; Dong, W.K. Tri- and hexanuclear heterometallic Ni(II)–M(II) (M = Ca, Sr and Ba) bis(Salamo)-type complexes: Synthesis, structure and fluorescence properties. *RSC Adv.* **2017**, *7*, 48394–48403. [CrossRef]
37. Peng, Y.D.; Li, X.Y.; Kang, Q.P.; An, G.X.; Zhang, Y.; Dong, W.K. Synthesis and fluorescence properties of asymmetrical Salamo-type tetranuclear zinc(II) complex. *Crystals* **2018**, *8*, 107. [CrossRef]
38. Li, X.Y.; Kang, Q.P.; Liu, L.Z.; Ma, J.C.; Dong, W.K. Trinuclear Co(II) and mononuclear Ni(II) Salamo-type bisoxime coordination compounds. *Crystals* **2018**, *8*, 43. [CrossRef]

39. Akine, S.; Tadokoro, T.; Nabeshima, T. Oligometallic template strategy for synthesis of a macrocyclic dimer-type octaoxime ligand for its cooperative complexation. *Inorg. Chem.* **2012**, *51*, 11478–11486. [CrossRef] [PubMed]
40. Nabeshima, T.; Akine, S.; Ikeda, C.; Yamamura, M. Metallo-supramolecular systems for synergistic functions based on unique arrangement of ligation sites. *Chem. Lett.* **2010**, *39*, 10–16. [CrossRef]
41. Akine, S.; Nabeshima, T. Cyclic and acyclic oligo(N_2O_2) ligands for cooperative multi-metal complexation. *Dalton Trans.* **2009**, *47*, 10395–10408. [CrossRef] [PubMed]
42. Dong, X.Y.; Gao, L.; Wang, F.; Zhang, Y.; Dong, W.K. Tri- and mono-nuclear zinc(II) complexes based on half- and mono-Salamo chelating ligands. *Crystals* **2017**, *7*, 267. [CrossRef]
43. Dong, W.K.; Ma, J.C.; Zhu, L.C.; Zhang, Y. Nine self-assembled nickel(II)-lanthanide(III) heterometallic complexes constructed from a Salamo-type bisoxime and bearing N- or O-donor auxiliary ligand: Syntheses, structures and magnetic properties. *New J. Chem.* **2016**, *40*, 6998–7010. [CrossRef]
44. Wang, L.; Ma, J.C.; Dong, W.K.; Zhu, L.C.; Zhang, Y. A novel self–assembled nickel(II)–cerium(III) heterotetranuclear dimer constructed from N_2O_2-type bisoxime and terephthalic acid: Synthesis, structure and photophysical properties. *Z. Anorg. Allg. Chem.* **2016**, *642*, 834–839. [CrossRef]
45. Dong, W.K.; Ma, J.C.; Dong, Y.J.; Zhu, L.C.; Zhang, Y. Di- and tetranuclear heterometallic 3d-4f cobalt(II)-lanthanide(III) complexes derived from a hexadentate bisoxime: Syntheses, structures and magnetic properties. *Polyhedron* **2016**, *115*, 228–235. [CrossRef]
46. Hao, J.; Li, L.H.; Zhang, J.T.; Akogun, S.F.; Wang, L.; Dong, W.K. Four homo- and hetero-bismetallic 3d/3d-2s complexes constructed from a naphthalenediol-based acyclic bis(Salamo)-type tetraoxime ligand. *Polyhedron* **2017**, *134*, 1–10. [CrossRef]
47. Gao, L.; Liu, C.; Wang, F.; Dong, W.K. Tetra-, penta- and hexa-coordinated transition metal complexes constructed from coumarin-containing N_2O_2 ligand. *Crystals* **2018**, *8*, 77. [CrossRef]
48. Percy, G.; Thornton, D. Infrared spectra of N-aryl salicylaldimine complexes substituted in both aryl rings. *J. Inorg. Nucl. Chem.* **1973**, *35*, 2319–2327. [CrossRef]
49. Dong, W.K.; Ma, J.C.; Zhu, L.C.; Zhang, Y. Self-assembled zinc(II)-lanthanide(III) heteromultinuclear complexes constructed from 3-MeO Salamo ligand: Syntheses, structures and luminescent properties. *Cryst. Growth Des.* **2016**, *16*, 6903–6914. [CrossRef]
50. Addison, A.W.; Rao, T.N.; Reedijk, J.; Rijn, J.V.; Verschoor, G.C. Synthesis, structure, and spectroscopic properties of copper(II) compounds containing nitrogen–sulphur donor ligands; the crystal and molecular structure of aqua [1,7-bis(*N*-methylbenzimidazol-2*0*-yl)-2,6-dithiaheptane]copper(II) perchlorate. *J. Chem. Soc. Dalton Trans.* **1984**, *7*, 1349–1356. [CrossRef]
51. Liu, Y.A.; Wang, C.Y.; Zhang, M.; Song, X.Q. Structures and magnetic properties of cyclic heterometallic tetranuclear clusters. *Polyhedron* **2017**, *127*, 278–286. [CrossRef]
52. Constable, E.C. Expanded ligands-An assembly principle for supramolecular chemistry. *Coord. Chem. Rev.* **2008**, *252*, 842–855. [CrossRef]
53. Chai, L.Q.; Li, Y.X.; Chen, L.C.; Zhang, J.Y.; Huang, J.J. Synthesis, X-ray structure, spectroscopic, electrochemical properties and DFT calculation of a bridged dinuclear copper(II) complex. *Inorg. Chim. Acta* **2016**, *444*, 193–201. [CrossRef]
54. Sun, Y.X.; Li, C.Y.; Yang, C.J.; Zhao, Y.Y.; Guo, J.Q.; Yu, B. Two Cu(II) complexes with schiff base ligands: Syntheses, crystal structures, spectroscopic properties, and substituent effect. *Chin. J. Inorg. Chem.* **2016**, *32*, 327–335.
55. Li, J.; Zhang, H.X.; Chang, J.; Jia, H.R.; Sun, Y.X.; Huang, Y.Q. Solvent-induced unsymmetric Salamo-like trinuclear Ni^{II} complexes: Syntheses, crystal structures, fluorescent and magnetic properties. *Crystals* **2018**, *8*, 176. [CrossRef]
56. Sun, Y.X.; Zhao, Y.Y.; Li, C.Y.; Yu, B.; Guo, J.Q.; Li, J. Supramolecular cobalt(II) and copper(II) complexes with schiff base ligand: Syntheses, characterizations and crystal structures. *Chin. J. Inorg. Chem.* **2016**, *32*, 913–920.
57. Liu, P.P.; Wang, C.Y.; Zhang, M.; Song, X.Q. Pentanuclear sandwich-type Zn^{II}-Ln^{III} clusters based on a new Salen-like salicylamide ligand: Structure, near-infrared emission and magnetic properties. *Polyhedron* **2017**, *129*, 133–140. [CrossRef]

58. Chen, Y.; Mao, S.S.; Shi, X.K.; Shen, K.S.; Wu, H.L. Synthesis, crystal structure, DNA-binding properties and antioxidant activity of a copper(II) complex with naphthalimide Schiff base. *Z. Anorg. Allg. Chem.* **2017**, *643*, 1182–1190. [CrossRef]
59. Shi, X.K.; Mao, S.S.; Shen, K.S.; Wu, H.L.; Tang, X. Synthesis, crystal structure, antioxidation and fluorescence of two lanthanide complexes with a noncyclic polyether Schiff base ligand. *J. Coord. Chem.* **2017**, *70*, 2015–2028. [CrossRef]